Cell Prolif. 2007, **40**, 338–354

Mathematical model for chemotherapeutic drug efficacy in arresting tumour growth based on the cancer stem cell hypothesis

R. Ganguly*'† and I. K. Puri*

**Department of Engineering Science and Mechanics, Virginia Polytechnic Institute and State University, Blacksburg, VA, USA, and †Department of Power Engineering, Jadavpur University, Kolkata, India*

Received 12 *September* 2006*; revision accepted* 25 *November* 2006

Abstract. *Objective*: Cancer stem cells have been identified as the growth root for various malignant tumours and are thought to be responsible for cancer recurrence following treatment. *Materials and methods*: Here, a predictive mathematical model for the cancer stem cell hypothesis is used to understand tumour responses to chemotherapeutic drugs and judge the efficacy of treatments in arresting tumour growth. The impact of varying drug efficacies on different abnormal cell populations is investigated through the kinetics associated with their decline in response to therapy. *Results and conclusions*: The model predicts the clinically established 'dandelion phenomenon' and suggests that the best response to chemotherapy occurs when a drug targets abnormal stem cells. We compare continuous and periodic drug infusion. For the latter, we examine the relative importance of the drug cell-kill rate and the mean time between successive therapies, to identify the key attributes for successful treatment.

INTRODUCTION

According to the cancer stem cell hypothesis, just as mature cells in some systems are maintained by self-renewing stem cells, malignant tumours occur through mutations of healthy stem and early progenitor cells, in the corresponding abnormal cells (Al-Hajj & Clarke 2004; Clarke 2004). Thus, understood, tumours consist of progeny of abnormal stem or progenitor cells (Reya *et al*. 2001; Pardal *et al*. 2003; Clarke 2004; Singh *et al*. 2004). A key contention of the hypothesis is that only a small subset of tumour cells has the ability to proliferate rapidly in many types of cancer. Consequently, because it is likely that cancerous stem cells are often responsible for recurrences that occur after conventional treatment, treatments must target cancer stem cells in order to eliminate the disease.

The transformation of stem cells into a malignant phenotype requires fewer mutations than are required to ectopically activate a more differentiated cell. Because stem cells are self-renewing

Correspondence: Ishwar K. Puri, Department of Engineering Science and Mechanics, Virginia Polytechnic Institute and State University, 231 Norris Hall (mc 0219) Blacksburg, VA 24061, USA. Tel.: (540)231 3243; Fax: (540) 231 4574; E-mail: ikpuri@vt.edu

they often persist for longer periods and are thus more likely to accumulate mutations than a shorter-lived progenitor or differentiated cell. Such progenitor cells inheriting mutations from a stem cell can also itself undergo further mutations to cause transformation. Malignant cells that arise after such mutations disrupt normal signalling pathways and usurp the self-renewal machinery that is normally the property only of stem cells. Consequently, many pathways associated with normal stem cell renewal are also implicated in oncogenesis, for example, Bmi-1 (Lessard & Sauvageau 2003; Molofsky *et al*. 2003), Sonic Hedgehog (Taipale & Beachy 2001) and Wnt (Polakis 2000; Taipale & Beachy 2001). The literature cites several techniques for mathematical modeling of haematopoietic, neural and embryonic stem cells (Viswanathan & Zandstra 2003), plus for cells of chronic myeloid leukaemia (CML) (Komarova & Wadarz 2005; Michor *et al*. 2005; Roeder *et al*. 2006). We (Ganguly & Puri 2006) have previously extended a compartmental method (Wichmann & Loeffler 1984) to formulate a predictive mechanistic mathematical model for a process based on a cancer stem cell hypothesis (Reya *et al*. 2001; Al-Hajj & Clarke 2004; Clarke 2004; Singh *et al*. 2004).

Ineffective targeting of the abnormal stem cell population within tumours can lead to therapeutic failures and cancer recurrence (Al-Hajj *et al*. 2004; Polyak & Hahn 2006). Most cytotoxic chemotherapeutic agents target the more rapidly proliferating progenitor cells during the cancer cell transit amplification stage (in which progenitor or amplifying cells expand the differentiating cell population through a series of symmetric divisions, Mackenzie 2005). Therefore, it is possible that the slower proliferating cancer stem cells can survive these treatments.

Our objective herein is to characterize tumour cell responses to chemotherapeutic drugs. We consider impact of different drug efficacies on various abnormal cell populations by observing the kinetics (e.g. imposed by the cell-kill rate) associated with their reduction in response to therapy. Such observations can help provide insight into disease responsiveness and resistance (Huntly & Gilliland 2005; Michor *et al*. 2005). Overall efficacies of continuous and periodic drug therapy in arresting tumour growth are compared and different modes of drug infusion and their outcomes are also examined. Finally, the relative importance of the cell-kill rate is demonstrated through a parametric study. These results could assist clinicians by providing comparative information on several possible chemotherapy modes and by identifying the key attributes of a successful therapy.

THE MODEL

Our model is schematically described in Fig. 1(a). It consists of two pathways, one normal and the other an abnormal path that occurs due to stem and early progenitor cell mutations. It is based on an evolutionary perspective, which assumes that cells regularly undergo mutations in their DNA. While the vast majority of these mutations are detrimental to cell survival, some cells, particularly those capable of self-renewal, infrequently survive the mutations. They subsequently drive the formation and pathology of the neoplasia (Clarke 2004). The model incorporates the role of internal cell signalling during proliferation. Hence, it is self-regulating; that is, normal cell signalling limits healthy cell proliferation to a steady value that is sufficient to replenish any steady death (apoptosis) of mature cells.

Other than tissue evasion and metastasis (since it does not consider cell transport), the model accounts for the remaining five hallmarks of malignancy (Hanahan & Weinberg 2000), These include (i) self-sufficiency in growth signals, (ii) insensitivity to antigrowth signals (which taken together represent the loss of regulation and signalling in abnormal cells), (iii) limitless replicative potential (i.e. the basis of the cancer stem cell hypothesis), (iv) acquisition of resistance to apoptosis and (v) sustained angiogenesis (here, we can incorporate different carrying capacities for the

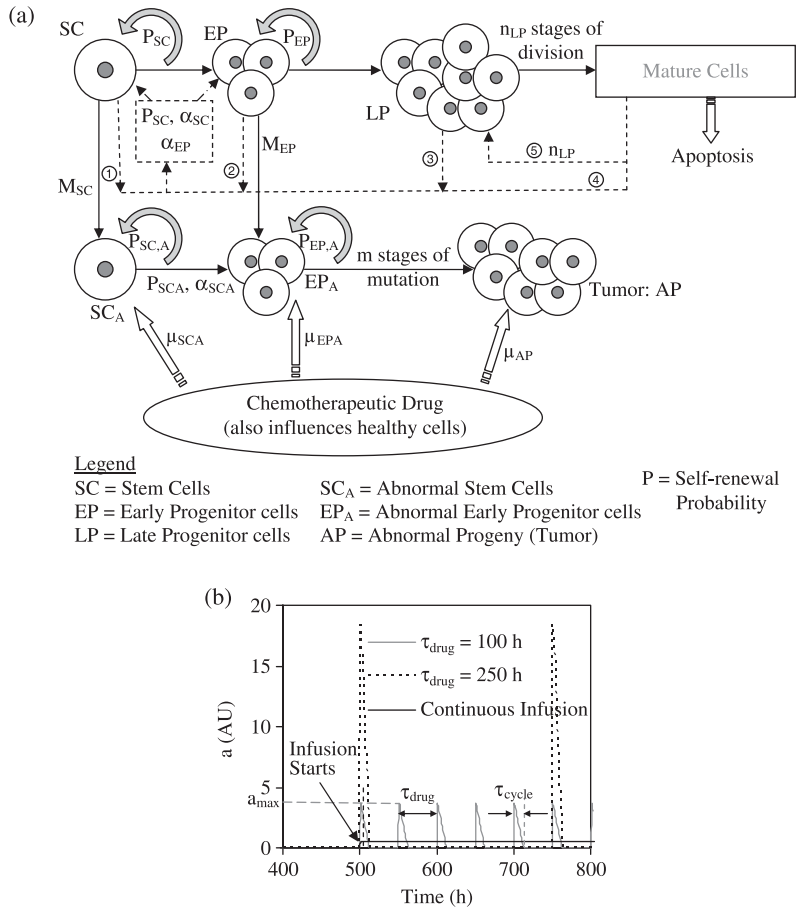

Figure 1. (a) Cancer stem cell model showing the cell-signalling pathway, and the action of a chemotherapeutic drug. (b) Instantaneous infusion rate 'a' for different modes of chemotherapeutic drug dosing, that is, continuous infusion, periodic infusion. Here, τ_{drug} denotes the time period between two consecutive drug doses, τ_{cycle} the duration of non-zero infusion rate in a cycle, and a_{max} the instantaneous peak infusion rate.

healthy and abnormal cell populations). We have previously used the model to confirm that mutations leading to malignant change are more significant when they occur in stem cells than in early progenitor cells. We have concluded in that investigation that cancer risk increases with increasing frequency of injury, for example, with a repeated insult that depletes the mature cell population (Ganguly & Puri 2006). While the model was deterministic (not stochastic), randomness could be readily included by changing various parameters [such as those reported in Tables 1 and 2 of Ganguly & Puri (2006)].

Cell fate choices in the model are assumed to arise from soluble signals that establish a concentration gradient. This enables cells within the gradient to adopt alternate, 'all-or-none' fates at critical threshold signal levels (Jessel & Lumsden 1997; O'Neill & Schaffer 2004). We assume that the concentration gradient becomes negligible when the mature cell population reaches a desired sustainable level (there is an upper signalling threshold). The growth mechanisms and factors influencing stem cell self-renewal are considered to be the same for both normal and abnormal stem cells (Oliver & Wechsler-Reya 2004). Thus, self-renewal probabilities for both

Table 1. Parameters used in the model

Parameter	Ssymbls	Values
Cell cycle time for SC, EP, LP compartments	τ_{SC}, τ_{EP}, τ_{LP}	12 h
Cell maturation time for LP compartment	τ_m	40 h
Self-renewal probability upper and lower limits for SC	$P_{max,SC}$, $P_{min,SC}$	0.6, 0.4
Self-renewal probability upper and lower limits for EP	$P_{max,EP}$, $P_{min,EP}$	0.5, 0.5
Upper and lower limits of mitotic fractions for stem cells	$\alpha_{max,SC}$, $\alpha_{min,SC}$	1, 0.01
Upper and lower limits of mitotic fractions for EP cells	$\alpha_{max,EP}$, $\alpha_{min,EP}$	1, 0.3
Number of EP cell self-renewals	k	5
Upper and lower limits of the number of mitotic cycles	$n_{LP,max}$, $n_{LP,min}$	3, 9
Death rate (apoptosis) of MC	$\dot{\omega}_{0,MC}$ (in AU)	0.01
Death Rate (apoptosis) of AP	$\dot{\omega}_{0,AP}$ (in AU)	0.01
Carrying capacity of healthy and abnormal cells	$\Theta_{healthy\ cells}$, Θ_a (in AU)	1000, 100
Rate at which drug becomes ineffective due to cell kill	γ (in AU)	0.01 for healthy cells 0.05 for abnormal cells
Drug decay rate	λ (in AU)	0.01
Duration of infusion in one therapy cycle	τ_{cycle}	25 h
Peak infusion rate	a_{max} (in AU)	0.5

Table 2. SCA and AP size at t = 2000 h expressed as percentages of their corresponding populations in absence drug therapy (a_{max} = constant)

	SCA	AP
$\tau_{drug} = \infty$	100	100
τ_{drug} = 500 h	85.7	85.1
τ_{drug} = 100 h	43.1	46.8
τ_{drug} = 25 h	11.6	14.9
$\tau_{drug} = 0$	5.6	8.5

normal and abnormal (or mutated) stem cells are identical, as are those for normal and abnormal early progenitor cells.

Stem cells (SC) are assumed to self-renew an unlimited number of times (Al-Hajj & Clarke 2004) with a self-renewal probability P_{SC}. Those that do not self-renew, differentiate to form early progenitor cells (EP). The self-renewal probability varies between a maximum $P_{max,SC}$ and a minimum $P_{min,SC}$ depending on the stem cell, and early and late progenitor cell (LP) populations. Self-renewal probability of early progenitor cells P_{EP} likewise lies between $P_{max,EP}$ and $P_{min,EP}$ depending on their respective cell populations. The model constrains early progenitor cells to self-renew a limited number of times *k* (Al-Hajj & Clarke 2004). Late progenitor cells undergo n_{LP} stages of cell division and produce mature cells (MC). Cell division regulatory feedback signalling controls the number of cell division stages between $n_{LP,min}$ and $n_{LP,max}$. A regulatory signal is responsible for maintaining a steady population of mature cells. The mature cell population also provides feedback to the stem cells thereby influencing their mitotic fraction and self-renewal rate. Regulatory feedback signals are represented by dotted lines that are numbered j through n in Fig. 1(a) [for which the mathematical representations are summarized in Table 2 of Ganguly & Puri (2006)].

The probabilities M_{SC} and M_{EP} represent occurrence of oncogenic mutation during DNA transcription for each cell division event involving stem cells or early progenitor cells. If mutation occurs, one daughter cell acquires the mutated gene following cell division while the other retains

the original DNA. Thus mutation of SC leads to formation of abnormal stem cells (SCA). Abnormal early progenitor cells can be formed either due to mutation in EP cells, or through differentiation of SCA. Subsequent differentiation of EPA leads to formation of abnormal progeny (AP). In our model, this AP population is the precursor of malignancy. Any increase or reduction in its size is presumed to be an equivalent increase or decrease of the risk of malignancy. Cancer arises when a cell with a mutated gene acquires the ability to proliferate indefinitely through the accumulation of at least C mutations. Due to uncontrolled proliferation, thereafter the associated cell cluster produces a malignant tumour (Reya *et al*. 2001). We consider each cell type as a separate compartment that has an individual rate expression for its cell population growth. The model also considers rates of apoptosis $\dot{\omega}_{0,MC}$ and $\dot{\omega}_{0,AP}$ for MC and AP, respectively.

CHEMOTHERAPEUTIC TREATMENT

It is possible to design chemotherapeutic drugs with selective efficacies towards different cell populations. Hence, we assume that when a drug is supplied it influences a particular cell sub-compartment with a specific efficacy. We therefore have assigned separate cell-kill rates μ for different healthy and abnormal cell compartments to account for this selectivity. This assumption is consistent with previous observations, for example, imatinib inhibits more than 90% of CML progenitor cell growth *in vitro* in the 1–10 μM concentration range but shows little activity against normal haematopoietic progenitors (Huff *et al*. 2006).

MATHEMATICAL DETAILS

The basic model for healthy and cancer stem cell pathways is described by Ganguly & Puri (2006). In this paper, the effect of a chemotherapeutic drug on the cell population equation is included in terms of its cell-kill rate μ. Each cell type has also been assumed to have its own carrying capacity Θ [an upper limit to which cell growth is limited, for example, by a bounded nutrient supply rate to the growing cell population, Byrne (2003)]. Thus, the cell proliferation relation accounting for drug therapy is

$$dN/dt = \dot{\omega}N(1 - N/\Theta) - \mu AN \tag{1}$$

where N denotes the cell population, $\dot{\omega} = (\alpha/\tau)\ln(2)$ the cell division rate (where α is the proliferative fraction and τ the cell cycle time). The average drug concentration A is determined from the expression

$$dA/dt = a(t) - \lambda A - \gamma AN \tag{2}$$

Equation (2) indicates that the net rate of change of drug concentration in a cellular matrix is a function of the drug infusion rate a(t), the natural drug decay (due to chemical decomposition of the drug or its transport, both associated with the decay rate λ) and the rate γAN at which the drug becomes ineffective due to cell-kill rate. The last terms in Equations (1) and (2) are related but γ and μ can have different numerical values. With the modification described in Equation (1), the rate of change in a cell population is also modified as follows.

Healthy cell compartments

For all healthy cell compartments (depicted on the upper pathway of the schematic diagram in Fig. 1a), an average cell-kill rate $\mu_{\text{healthy cells}}$ and an average carrying capacity Θ_H are assumed.

Stem cell compartment (*population* N_{SC}):

$$\frac{dN_{SC}}{dt} = \dot{\omega}_{SC}(2P_{SC} - 1 - M_{SC})\left(1 - \frac{N_{SC}}{\Theta_H}\right)N_{SC} - \mu_{\text{healthy cells}}AN_{SC} \tag{3}$$

Early progenitor compartment (*consisting of k sub-compartments, each with a population* N_{EP_i}):

$$\frac{dN_{EP_1}}{dt} = 2\dot{\omega}_{SC}(1 - P_{SC})\left(1 - \frac{N_{SC}}{\Theta_H}\right)N_{SC} - \dot{\omega}_{EP}\left(1 - \frac{N_{EP_1}}{\Theta_H}\right)N_{EP_1} - \mu_{\text{healthy cells}}AN_{EP_1} \tag{4a}$$

$$\frac{dN_{EP_i}}{dt} = \dot{\omega}_{EP}(2P_{EP_{i-1}} - M_{EP})\left(1 - \frac{N_{EP_{i-1}}}{\Theta_H}\right)N_{EP_{i-1}} - \dot{\omega}_{EP}\left(1 - \frac{N_{EP_i}}{\Theta_H}\right)N_{EP_i} - \mu_{\text{healthy cells}}AN_{EP_i}$$

(for i = 2 ... k) (4b)

Total efflux of differentiated EP cells that enter the LP compartment:

$$\dot{N}_{EP}^{\text{out}} = \sum_{i=1}^{k-1} 2\dot{\omega}_{EP}(1 - P_{EP})\left(1 - \frac{N_{EP_i}}{\Theta_H}\right)N_{EP_i} + 2\dot{\omega}_{EP}\left(1 - \frac{N_{EP_k}}{\Theta_H}\right)N_{EP_k} \tag{5a}$$

$$\text{Efflux of mutated EP cells} = \sum_{i=1}^{k-1} \dot{\omega}_{EP}\left(1 - \frac{N_{EP_i}}{\Theta_H}\right)M_{EP}N_{EP_i} \tag{5b}$$

Late progenitor cell compartment (*population* N_{LP}):

$$\frac{dN_{LP}}{dt} = Z^{\text{in}}\dot{N}_{EP}^{\text{out}} - \dot{\omega}_{LP}\left(1 - \frac{N_{LP}}{\Theta_H}\right)N_{LP} - \mu_{\text{healthy cells}}AN_{LP} \tag{6a}$$

where $Z^{\text{in}} = \{(2^{n_{LP}} - 1)\tau_g/\tau_{LP} + 2^{n_{LP}}\tau_m/\tau_{LP}\}$ and $Z^{\text{in}} \times Z^{\text{out}} = 2^{n_{LP}}$ and τ_g (= $\tau_{LP}/\alpha_{LP}\ln 2$) and τ_m denote cell generation time and cell maturation time, respectively (Ganguly & Puri 2006).

$$\text{Efflux from the LP compartment } \dot{N}_{LP}^{\text{out}} = Z^{\text{out}}\dot{\omega}_{LP}\left(1 - \frac{N_{LP}}{\Theta_H}\right)N_{LP} \tag{6b}$$

Mature cell compartment (*population* N_{MC}):

$$\frac{dN_{MC}}{dt} = \dot{N}_{LP}^{\text{out}} - \dot{\omega}_{0,MC}N_{MC} - \mu_{\text{healthy cells}}AN_{MC} \tag{7}$$

Abnormal stem cell compartment

Following Ganguly & Puri (2006), abnormal stem cells are assumed to have the same self-renewal rates P_{SC} and proliferative fractions (therefore, the same values of $\dot{\omega}_{SC}$) as their healthy counterparts. Similarly, abnormal EP cells also have the same values of P_{EP} and $\dot{\omega}_{EP}$ as healthy EP cells. For the abnormal cell population, the drug is assumed to have selective kill rates μ_{SCA}, μ_{EPA}, and μ_{AP}, respectively. A separate carrying capacity Θ_a is considered for the abnormal cells.

Abnormal stem cell compartment:

$$\frac{dN_{SCA}}{dt} = \dot{\omega}_{SC}(2P_{SC} - 1)\left(1 - \frac{N_{SCA}}{\Theta_a}\right)N_{SCA} + \dot{\omega}_{SC}\left(1 - \frac{N_{SC}}{\Theta_H}\right)M_{SC}N_{SC} - \mu_{SCA}AN_{SCA} \quad (8)$$

Abnormal early progenitor cell compartment:

$$\frac{dN_{EPA_1}}{dt} = 2\dot{\omega}_{SC}(1 - P_{SC})\left(1 - \frac{N_{SCA}}{\Theta_a}\right)N_{SCA} - \dot{\omega}_{EP}\left(1 - \frac{N_{EPA_1}}{\Theta_a}\right)N_{EPA_1} - \mu_{EPA}AN_{EPA_1} \quad (9a)$$

$$\frac{dN_{EP_i}}{dt} = 2P_{EPA_{i-1}}\dot{\omega}_{EP}\left(1 - \frac{N_{EPA_{i-1}}}{\Theta_a}\right)N_{EPA_{i-1}} - \dot{\omega}_{EP}\left(1 - \frac{N_{EPA_i}}{\Theta_a}\right)N_{EPA_i} + M_{EP}\dot{\omega}_{EP}\left(1 - \frac{N_{EP_i}}{\Theta_{\text{healthy cells}}}\right)N_{EP_i} - \mu_{EPA}AN_{EPA_i} \quad \text{for } i = 2 \ldots k \quad (9b)$$

The efflux of abnormal EP cells

$$\dot{N}_{EPA}^{out} = \sum_{i=1}^{k-1} 2\dot{\omega}_{EP}(1 - P_{EP})\left(1 - \frac{N_{EPA_i}}{\Theta_a}\right)N_{EPA_i} + 2\dot{\omega}_{EP}\left(1 - \frac{N_{EPA_k}}{\Theta_a}\right)N_{EPA_k} \quad (10)$$

Abnormal progeny compartment:

$$\frac{dN_{AP}}{dt} = \dot{N}_{EPA}^{out} - \dot{\omega}_{0,AP}N_{AP} - \mu_{AP}AN_{AP} \quad (11)$$

DISCUSSION

Equations (2) through (11) were numerically solved using a time marching scheme, and the parameters specified in Table 1 of Ganguly & Puri (2006). The model has previously been tested by Ganguly & Puri (2006) for its stability and steady state response. We have demonstrated that SC mutations have a much larger proliferation potential than mutations in EP cells. Thus, mutations leading to malignancy are more significant when they occur in stem cells than in early progenitor cells. The model predicts that repeated insult increases the proportion of the stem cell population that participates in cell division thereby enhancing the growth rate of abnormal progeny.

Here, we have modeled the effects of both the continuous and of the periodic infusion of a drug on (healthy and abnormal) cells. During continuous infusion, drug dose is constant over the entire duration of chemotherapy. During periodic dosing, drug infusion occurs every τ_{drug} hours and, consequently, the instantaneous drug concentration decays due to inactivation both through cell kill and to the natural decay of the drug. Perhaps, the simplest representation of temporal drug decay is through the saw-tooth curve described schematically in Fig. 1(b), which we have incorporated into our model.

We have considered various periodic dosing times τ_{drug}. Drug infusion is initiated every τ_{drug} hours with a maximum infusion rate a_{max} that linearly decreases to 0 after τ_{cycle} hours. In order to analyze chemotherapeutic effects at different dosing frequencies, a_{max} can either be held constant irrespective of the value of τ_{drug} or it can be assumed to have an inverse relationship with it. In the latter case, the total amount of infused drug ($a^* = \int a\,dt$) is conserved over a specified treatment

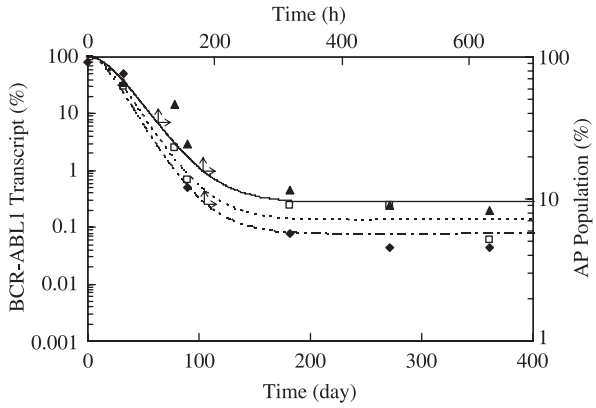

Figure 2. Response of the BCR-ABL1 transcript levels in imatinib-treated CML cases (the experimental data ◆ and ▲ are from Michor *et al*. 2005; □ is from Roeder *et al*. 2006). Our model (plotted against the secondary axis) also predicts a similar biphasic response using different cell-kill rates (that are analogues of the parameter r_{deg} in Roeder *et al*. 2006), that is, $\mu_{SCA} = 0.3$, — · — $\mu_{SCA} = 0.4$, ·····; and $\mu_{SCA} = 0.5$, ——.

time, that is, the same total dose is always infused irrespective of the dosing frequency. For the former type of periodic dosing (when a_{max} is maintained constant), a* is not conserved but is inversely proportional to τ_{drug}. In this case, the more frequent the dosing the larger the value of a*. Figure 1(b) illustrates three drug infusion models for which a* is conserved, one of which is continuous and the other two are periodic with values of τ_{drug} = 100 h and 250 h.

The overall drug efficacy is characterized through its effect on abnormal progeny size. Here, we have assumed that the size of a like cell mass is proportional to the cell population within a compartment. The dynamic response of our model is compared to experimental results of Michor *et al*. (2005) and Roeder *et al*. (2006). These teams have found that successful therapy exhibits a biphasic exponential decline in leukaemic cells in imatinib-treated CML. Experimental data (◆, □ and ▲) in Fig. 2 demonstrate the heterogeneous response of the BCR-ABL1 transcript levels. The primary effect (exhibited through a steep decline) was induced by initial reduction of proliferating BCR-ABL1-positive cells due to the assumed degradation effect. The later moderate decline was largely based on changes in regulatory response of the system due to reduced stem cell numbers. Roeder *et al*. (2006) successfully modeled this effect by assuming different values of imatinib-induced degradation, r_{deg}. The closest analogue to the parameter r_{deg} in our model is the cell-kill rate, μ_{SCA}. Results from our model presented in Fig. 2 predict a similar response for AP cells under continuous infusion for three different μ_{SCA} values ($\mu_{SCA} = 0.5$, — · —; $\mu_{SCA} = 0.4$, ·····; and $\mu_{SCA} = 0.5$, ——). Consistent with the experiments, the simulations show an initially rapid decline in AP cell population that is followed by a slower response. Results presented in Fig. 2 clearly suggest that our model predictions are consistent with clinically determined trends for chemotherapeutic response in imatinib-treated CML cases.

Figure 3 depicts the response of the AP size to therapy. We have assumed that after a tumour is detected, therapy is initiated at 500 h and treatment continues until 2000 h. Both continuous and periodic infusion are examined with τ_{drug} = 100 h and τ_{cycle} = 25 h for the periodic case. Drug efficacies for the different abnormal cell populations are varied but the effect of the drug on healthy cells ($\mu_{healthy\ cells} = 0.01$ in arbitrary units, AU) is always the same.

The results show that the AP size diminishes by the largest extent when a drug has equally vigorous effects on the SCA, EPA and AP compartments (here $\mu_{SCA} = \mu_{EPA} = \mu_{AP} = 0.1$). However,

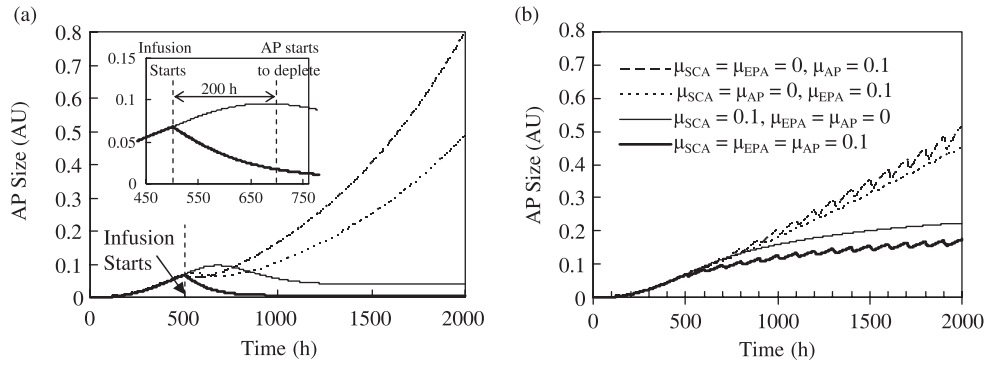

Figure 3. Effect of selective efficacy (represented in terms of the cell-kill rate, μ) of the chemotherapeutic drug on the abnormal progeny size. The panels show the growth rate of AP over time with (a) a continuous injection rate of 0.5 units, and (b) periodic infusion of $a_{max} = 0.5$ units. Each session of drug infusion occurs over $\tau_{cycle} = 25$ h, and the time period τ_{drug} between two consecutive infusions is 100 h. For both cases, $\mu_{healthy\ cells} = 0.01$. Drug infusion begins at t = 500 h. The inset in Fig. 3(a) shows an enlarged view of the response lag of the AP population to a drug that is selective to AP alone in comparison with one that is selective to SCA only. The legends for the curves are identical for Fig. 3(a), its inset, and for Fig. 3(b).

such equivalent effects of a drug on all three kinds of abnormal cell populations are not generally clinically feasible. Therefore, it is instructive to examine AP growth with different drug efficacies for the three abnormal populations. Figure 3 presents results when each of μ_{SCA}, μ_{EPA} and μ_{AP} are separately held at 0.1 with the other two values set to 0 (e.g. if $\mu_{SCA} = 0.1$ then μ_{EPA} and μ_{AP} are both 0 and so on). Overall drug efficacy is based on the AP size at 2000 h (i.e. after 1500 h of therapy). When $\mu_{SCA} = \mu_{EPA} = 0$ and $\mu_{AP} = 0.1$, the AP size is 0.80 AU with continuous injection and 0.51 AU for periodic injection. For the case $\mu_{SCA} = \mu_{AP} = 0$ and $\mu_{EPA} = 0.1$, these values are 0.49 and 0.45 AU, respectively. A marked reduction in the AP size (0.04 AU for continuous infusion, 0.22 AU for periodic infusion) occurs when $\mu_{SCA} = 0.1$ and $\mu_{EPA} = \mu_{AP} = 0$. There is very little improvement over these values (0.01 and 0.17 AU for continuous and periodic infusion, respectively) when $\mu_{SCA} = \mu_{AP} = \mu_{EPA} = 0.1$. These results indicate that AP growth is most inhibited when a drug acts on the abnormal stem cells regardless of the mode of drug infusion.

Figure 3(a) shows that drug response immediately following infusion is progressively more sluggish when the drug acts on EPA or SCA alone instead of on AP. For example, when $\mu_{AP} = 0.1$ (and $\mu_{SCA} = \mu_{EPA} = 0$) there is an immediate reduction in the AP size. In contrast, when the drug acts on the SCA compartment alone, the AP size continues to grow until ≈200 h following infusion. The inset of Fig. 3(a) shows that the AP population continues to grow from 0.068 AU at 500 h to 0.096 AU at t = 700 h before it starts to decline and eventually reduces to 0.012 AU at 2000 h. The delay in response of the AP population to the drug occurs because the amplification of the SCA population into AP transpires with its own time constant. Although targeting the SCA compartment produces a more sluggish initial response as compared to targeting AP cells, it ultimately has a much higher efficacy. This can be explained using the metaphor of the 'dandelion phenomena' (Jones *et al*. 2004; Huff *et al*. 2006). It logically states that in order to eliminate a dandelion both the stem (or visible portion) of the weed and its root must be removed. Therefore, therapies that offer the potential for the cure of cancers derived from stem cells must target the abnormal stem cells (i.e. the root) that are responsible for disease maintenance, because the elimination of mature cells (i.e. the stem) alone may not lead to a cure. This again explains the smaller overall efficacy of chemotherapy when AP cells instead of the SCA population are targeted by the drug.

As an example, breast tumours that exhibit a basal phenotype similar to healthy mammary progenitor cells are resistant to standard chemotherapy. This supports the hypothesis that therapeutic success in this case could depend on targeting cancer stem cells (Brenton *et al*. 2005). Imanitib was developed as part of a program to identify drugs that block unregulated activity of protein kinases in various types of cancers (Huff *et al*. 2006). It produces a rapid response in decreasing CML tumours due to its striking activity against CML progenitors (O'Brien *et al*. 2003). However, many of its early responses are not durable (Mauro *et al*. 2003; Cortes *et al*. 2004) because some CML patients relapse quickly when the drug is discontinued (Cortes *et al*. 2004) while others show evidence of progression despite continuing with the therapy (Mauro *et al*. 2003). This has been explained as CML stem cell resistance to Imanitib (Huff *et al*. 2006). On the other hand, primary activity of interferon may be confined to CML stem cells (Bonifazi *et al*. 2001), which produces a slow but often durable response in curbing CML (Pierce *et al*. 2001). because the rationale behind the cancer stem cell hypothesis is to identify the 'roots' of cancer and propose durable remedies, for the remainder of the discussion we will focus on drugs that have a specific selectivity towards the SCA population only.

We have noted that the AP population does not exhibit a 'saw-tooth' waveform during periodic drug infusion when $\mu_{AP} = 0$. When a drug does not act on the AP compartment, the AP population is solely controlled by the differentiation of EPA to AP and indirectly by the differentiation of SCA to EPA. Equation 11 (for the AP compartment) is a first order differential equation with a time-constant $\tau = 1/(\dot{\omega}_0 + \mu_{AP}A)$.[§] When $\mu_{AP} = 0$ and the AP death rate $\omega_0 = 0.01$, this time-constant is of the order of 100 h. Similar re-arrangements of Equation 9(a) and (b) reveal that the time-constant associated with each EPA sub-compartment is $\tau = 1/(\dot{\omega}_{EP} + \mu_{EPA}A)$. Considering $\mu_{EPA} = 0$ and $\dot{\omega} = (\alpha_{EP}/\tau_{EP})\ln 2$, the time-constant for EPA ranges from 17 to 57 h when α_{EP} lies in the range 1–0.3 (Refer to Table 1). Thus, with $\mu_{SCA} = 0.1$, and $\mu_{EPA} = \mu_{AP} = 0$, any variation in the SCA population with periodic dosing τ_{drug} is 'smoothened' as the fluctuation of the cell population propagates through k EPA sub-compartments before being reflected in the transient response of the AP population. On the contrary, when $\mu_{AP} = 0.1$ and the average drug concentration is 0.1 (as found from the simulations), the representative time-constant for the AP compartment is $\tau = 1/(0.01 + 0.1 \times 0.1) = 50$ h. Thus, any ripple in the cell population with a larger time period (e.g. in the case reported in Fig. 3b with $\tau_{drug} = 100$ h) is reflected in the form of a saw-tooth profile for the time-response curve of the AP population.

Effects of chemotherapy on abnormal as well as on healthy cell populations are portrayed in Figs 4 and 5 for different dosing frequencies. For all these cases, the drug is considered to have one order of magnitude lower cell-kill rate for healthy cells (i.e. $\mu_{SCA} = 0.1$ and $\mu_{\text{healthy cells}} = 0.01$). Therapy is again assumed to extend from 500 h to 2000 h. Two dosing modes are considered. First, the maximum drug-dosing rate a_{max} is specified – as in a case when a maximum tolerated dose that should not be exceeded is stipulated, in order to prevent systemic side effects (Mayer *et al*. 2006). For this type of dosing, the value of a* varies inversely with the dosing frequency.

Figure 4(a) presents the time-response of AP to therapies with different periodicity, that is, $\tau_{drug} = 25$ h, 100 h and 500 h. For all three cases $a_{max} = 0.5$ AU with each drug infusion session occurring over a period $\tau_{cycle} = 25$ h. For comparison, AP response to continuous infusion over the same duration and with an identical dosing rate (0.5 AU), and for the case when there is no therapy, are also presented. These latter two cases establish the theoretical lower and upper limits for τ_{drug} and are, respectively, 0 and ∞. The corresponding MC and SCA population are plotted

[§]If a first order system is represented by the equation $dx/dt = ax + bu$, where x is the dependent variable (the cell size in the present case), u the input function (input from the other cell compartments), and a and b are constants, then the time-constant of the system is $\tau = -1/a$.

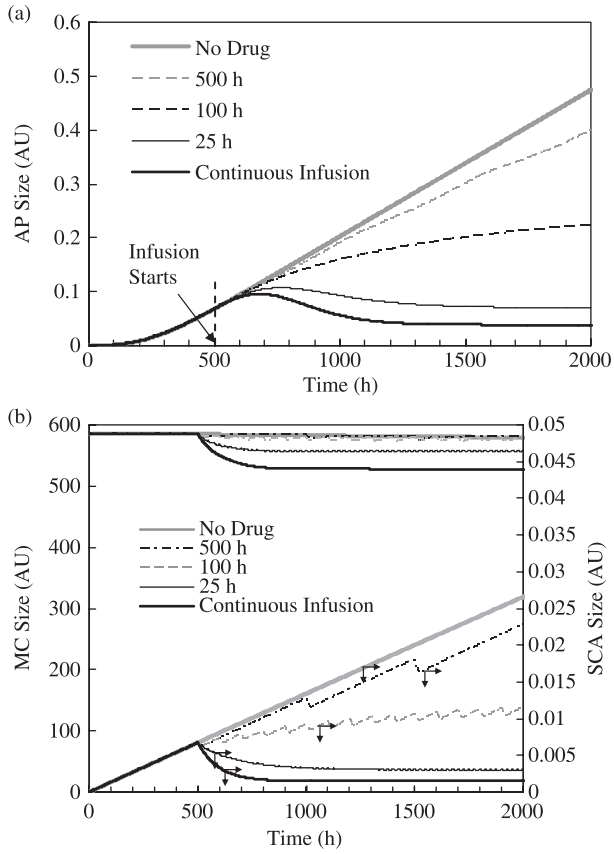

Figure 4. (a) Effect of drug infusion frequency on the AP size. The limiting cases are for no drug infusion ($\tau_{drug} = \infty$) and continuous drug infusion ($\tau_{drug} = 0$). Each drug infusion session occurs for 25 h with $a_{max} = 0.5$ units. $\mu_{SCA} = 0.1$, $\mu_{EPA} = \mu_{AP} = 0$, $\mu_{healthy\ cells} = 0.01$. (b) Corresponding variations in the MC and SCA populations. Drug infusion begins at t = 500 h.

in Fig. 4(b). Next, the same cases are examined when the total drug administered a* is conserved between 500 and 2000 h for all the values of τ_{drug} (except, of course, when $\tau_{drug} = \infty$ for which a* = 0). The corresponding responses of the SCA, MC and SCA populations are plotted in Fig. 5.

As shown in Fig. 4(a), the AP population at the beginning of drug infusion is 0.068 AU. When no drug is administered, it grows to 0.47 AU at 2000 h. Recall from Fig. 3(a) that the AP population reaches 0.80 AU when $\mu_{SCA} = \mu_{EPA} = 0$ and $\mu_{AP} = 0.1$ AU. This indicates that abnormal progeny size reduces significantly with chemotherapy that targets SCA cells instead of AP. Figure 4(a) indicates that the AP sizes (in AU) following 1500 h of chemotherapy are 0.47, 0.4, 0.22, 0.07 and 0.04 when $\tau_{drug} = \infty$ (i.e. when no drug is administered), 500 h, 100 h, 25 h and 0 h (or when there continuous infusion), respectively. This indicates that a_{max} being held constant, more frequent chemotherapy sessions have greater efficacy. Here, continuous infusion produces the best result, because consistent with intuition, the total amount of the dosed drug a* increases as τ_{drug} decreases.

The model considers the drug to have a low cell-kill rate with respect to healthy cells ($\mu_{healthy\ cells} = 0.01$), which leads to a steady depletion in the MC and other healthy cell populations. Any reduction in healthy cells from their equilibrium values stimulates regulatory feedback signals

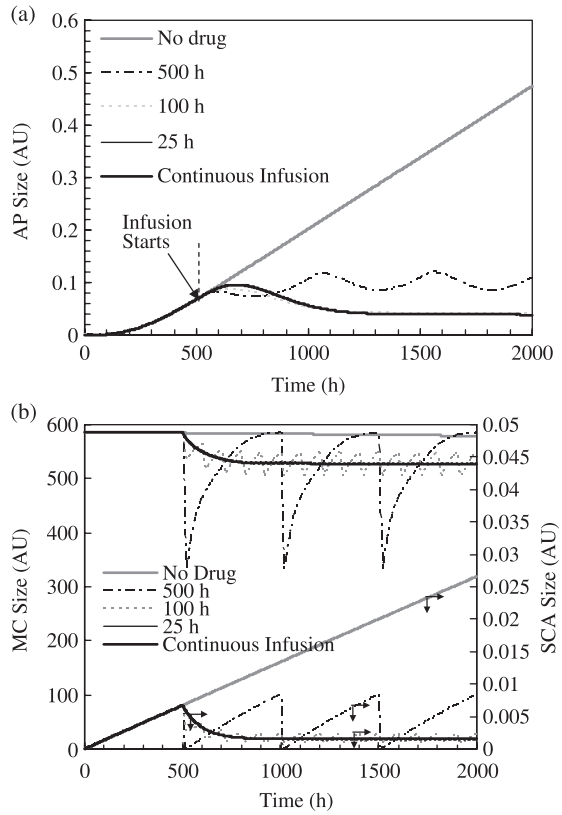

Figure 5. Effect of drug infusion frequency on the (a) AP number and (b) SCA and MC populations. The limiting cases are for no drug infusion ($\tau_{drug} = \infty$) and continuous drug infusion ($\tau_{drug} = 0$, a = 0.05 units). Each session of drug infusion occurs for 25 h. a_{max} is adjusted at different dosing frequencies such that $a^* = \int a \cdot dt$ is constant for all dosing frequencies. For all cases, $\mu_{SCA} = 0.1$, $\mu_{EPA} = \mu_{AP} = 0$, $\mu_{healthy\ cells} = 0.01$. Drug infusion begins at t = 500 h.

① through ⑤ (cf. Fig. 1a) and increases the SC (and therefore SCA) proliferation rates. This increase in the SCA population increases AP production, which could under certain conditions counterbalance abnormal progeny removal through chemotherapy. This indicates that a drug that targets AP cells alone can hypothetically exacerbate tumour treatment unless it has a large enough AP kill rate (i.e. a large value of μ_{AP}) or low enough side effects on healthy cells (with a low value for $\mu_{healthy\ cells}$).

Mature cells and SCA populations for these cases are presented in Fig. 4(b). Continuous infusion leads to a small depletion in the MC population from an equilibrium value of 578.8 AU to 527.8 AU. This 8.8% MC decrease induces SC (and SCA) proliferation through feedback signalling. Regardless, the SCA population does not exceed, for any τ_{drug} value, the corresponding value for the case when there is no treatment (because the drug now directly targets the SCA population). The SCA population diminishes immediately after the drug is administered. The greatest response is again observed for continuous infusion with which the SCA population reduces to 22% of its initial size. As before, the SCA population does not decline as rapidly for larger τ_{drug} values. After initially declining, SCA size actually increases slightly with time, indicating that cell-kill rate is lower than the SCA production rate when $\tau_{drug} > 100$ h. In contrast, for $\tau_{drug} > 500$ h SCA growth is only marginally arrested below the SCA build-up without drug therapy.

At 2000 h, SCA populations are respectively 0.0266, 0.0228, 0.0116, 0.0031and 0.0015 AU when $\tau_{drug} = \infty$, 500 h, 100 h, 25 h and 0 h. Table 2 presents final SCA and AP populations for different τ_{drug} values expressed as percentages of their respective sizes would have been in the absence of therapy. Correlation between the reduction in the AP and SCA populations under therapy is almost linear. AP behaviour, presented in Fig. 4(a), therefore follows a trend similar to the SCA activity in Fig. 4(b), but with a time-lag.

When total infusion a* is constant irrespective of τ_{drug}, the response of the AP population to chemotherapy is much different. As shown in Fig. 5(a), the AP population at 2000 h is 0.11, 0.04 and 0.04 AU when τ_{drug} = 500, 100 and 25 h, respectively. Drug efficacy does not noticeably alter when τ_{drug} changes. However, periodic infusion produces large transient declines in the MC population (Fig. 5b). For instance, the MC population decreases from 585.4 to 335.8 AU immediately following infusion during each cycle when τ_{drug} = 500 h. This is due to the large a_{max} value (cf. Fig. 1b) imposed as τ_{drug} increases so as to maintain a constant a* value. Therefore, when τ_{drug} = 100 h the MC depletion is smaller (from 585.4 to 509.6 AU). Because depletion of mature cells is an undesirable side effect of therapy, particularly for sensitive populations, the results imply that administering large doses at infrequent periods could be detrimental to patient health. For example, survivors of medulloblastoma show signs of impaired neuropsychological activity in the first decade after chemotherapy and radiation treatment (Maddrey *et al*. 2005), both of which have the deleterious side effect of healthy brain tissue damage.

So far, we have considered an arbitrarily chosen constant value of μ_{SCA} (= 0.1) for our analysis. However, different drugs may have varying SCA kill rates. Thus, it is important to investigate how variations in μ_{SCA} can alter the results of chemotherapy for both continuous and periodic infusions with different values for τ_{drug}. Figure 6 presents the AP population at t = 2000 h as function of μ_{SCA} when a_{max} and a* are held constant, respectively. As before, the drug is administered from t = 500 h to t = 2000 h, and all the other parameters (e.g. τ_{cycle}, $\mu_{healthy\ cells}$, etc.) are unchanged.

Figure 6(a) indicates that for a continuous infusion process, significant improvement in drug efficacy is achieved when the value of μ_{SCA} is raised by even a very small value above 0. The post-treatment AP size decreases by almost 95% from that in the absence of therapy when μ_{SCA} is raised from 0 to 0.12. However, further increase in μ_{SCA} does not alter efficacy as significantly and the final AP population is eventually almost insensitive to any further increases in μ_{SCA}. For τ_{drug} = 100 h, the effect of μ_{SCA} is less pronounced, because for μ_{SCA} = 0.5 the decline in AP size is 90.5% as compared to one in the absence of therapy. Unlike the case of continuous infusion, the AP versus μ_{SCA} curve continues to monotonically decrease within the range of the study. The slope of this curve decreases with increasing τ_{drug}. For example, with μ_{SCA} = 0.5, the AP sizes at t = 2000 h for τ_{drug} = 250 h, 500 h and 1000 h are 24%, 44% and 55% in comparison with the case when there is no therapy (Fig. 6a). Thus, when a_{max} = constant (i.e. a* is not conserved), a more vigorous drug is progressively less effective as the time between two consecutive infusion increases. On the contrary, when a* is conserved over the entire duration of therapy and μ_{SCA} is smaller than 0.04, the sensitivity of drug efficacy on μ_{SCA} at all τ_{drug} values is almost as satisfactory as that produced through continuous infusion.

Figure 6(b) indicates that increasing the value of μ_{SCA} from 0 to 0.04 can result in a more than 80% reduction in AP growth for all the τ_{drug} values considered here. Beyond a threshold of μ_{SCA} (0.3, 0.18, 0.12 and 0.06 for τ_{drug} = 100 h, 250 h, 500 h and 1000 h, respectively, as shown in the inset of Fig. 7b), AP size ceases to significantly deplete with any further increase in μ_{SCA}. This implies that for periodic therapy with conserved a*, an acceptable result is achieved when the drug has a threshold value of μ_{SCA}. A drug with a μ_{SCA} value lower than this threshold does not decrease the AP population to the maximum extent possible. In contrast,

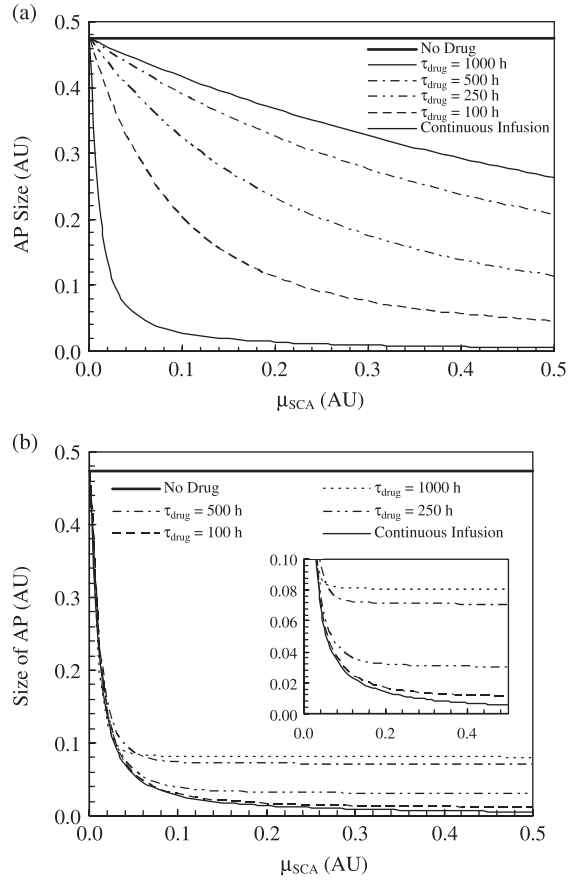

Figure 6. Efficacy of chemotherapy in diminishing the AP population as a function of the SCA kill rate μ_{SCA} for different drug infusion conditions: (a) a_{max} = constant for all frequencies and a* is not conserved, and (b) a_{max} is adjusted at different dosing frequencies so that a* is conserved. The plot indicates the AP size at t = 2000 h. Drug infusion occurs from t = 500 h to t = 2000h. The inset of Fig. 6(b) shows an enlarged view of the same plot.

while a larger value of μ_{SCA} could produce more pronounced side effects, it would provide no tangible improvement in efficacy, for example, through drug resistance (Stordal *et al*. 2006).

Continuous infusion yields better overall efficacy than periodic infusion. However, the latter is often the more feasible option from a mobility perspective. Nonetheless, there is a trade-off. While a large value of τ_{drug} is desirable from a convenience perspective, it has lower efficacy. Choosing a large value for μ_{SCA} may not necessarily compensate for a large τ_{drug} interval, because values above a threshold value of μ_{SCA} do not provide significant therapeutic improvement. Therefore, the combination of τ_{drug} and μ_{SCA} that is selected is important.

Figure 7 presents the results of a parametric simulation to determine the minimum μ_{SCA} required to achieve 95% reduction in AP as a function of τ_{drug}. Within the range 25 h < τ_{drug} < 250 h, this μ_{SCA} value increases monotonically for both the two conditions: (i) when a_{max} = constant and a* is not conserved and (ii) when a* is conserved. Thus, to achieve the same treatment efficacy, a larger τ_{drug} period requires a larger value of μ_{SCA}. It is apparent from Fig. 7 that the average slope of the curve for the condition when a* is not conserved is much higher than that for when a* is conserved. For the first case the required value of μ_{SCA} increases from 0.25 for τ_{drug} = 25 h

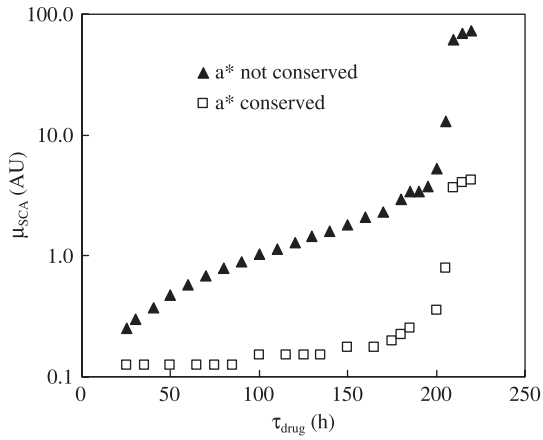

Figure 7. Drug efficacy in terms of the SCA cell kill rate, in AU, required to eradicate 95% of the SCA population plotted as a function of the time between two consecutive treatments during periodic drug infusion. For curve ▲, a_{max} is constant so that a* is not conserved. For curve □, a_{max} is adjusted such that a* is conserved. Chemotherapy begins at t = 500 h and continues until t = 2000 h. Each session of drug infusion occurs for 25 hours.

to 5.3 when τ_{drug} = 200 h. In contrast, this value increases from 0.125 when τ_{drug} = 25 h to 0.35 for τ_{drug} = 200 h when a* is conserved. Both plots exhibit sudden increase by almost one order of magnitude in the required μ_{SCA} values as τ_{drug} approaches 200 h, after which the curves plateau. This implies that it becomes chemotherapeutically challenging to control cancer if the time between two consecutive therapies exceeds 200 h for the specific conditions of our model. These results should be interpreted qualitatively because different therapeutic conditions applied in the model will yield other quantitative results.

CONCLUSIONS

Efficacy of chemotherapeutic drug therapy for cancer has been investigated using a predictive model based on the cell compartment method. Continuous and periodic drug infusions with different time periods between successive infusions were compared. The infused drug was considered to have either a constant maximum infusion rate a_{max} or a conserved total infusion quantity a*.

1 For both continuous and periodic infusions drug efficacy for controlling AP cells is greater when the drug acts selectively on SCA alone, rather than on EPA or AP alone.

2 When a drug acts on AP alone, the AP growth is immediately arrested. However, its longer-term efficacy is relatively poorer than if the drug had acted on other compartments. On the other hand, if the drug has a selective efficacy towards SCA alone, although the reduction in the AP cell population is delayed, it is more pronounced. Hence, targeting a drug selectively to remove SCA cells is preferable to targeting EPA or AP cells alone.

3 When a drug is administered periodically and the maximum dosing rate a_{max} is held constant (rather than the total infusion quantity a*) reduction in the AP population declines, as the time period τ_{drug} between consecutive therapies increases. At the upper limit, the higher efficacy is achieved for continuous infusion for which a* is also the largest.

4 If periodic infusion is performed, such that a* is conserved, drug efficacy is not as strongly affected by τ_{drug}. However, in case of large τ_{drug} values, instantaneous drug infusion rate a_{max}

must also be higher, leading to a large temporary decline in the healthy cell population due to side effects induced by the drug. Therefore, such a mode of therapy could be detrimental for populations more susceptible to side effects.

5 During continuous infusion, drug efficacy is very sensitive to μ_{SCA} values when these are relatively small. Post-treatment AP size decreases by almost 95% from that in the absence of therapy when μ_{SCA} is raised from 0 to 0.12. However, further increases in the values of μ_{SCA} do not alter the efficacy as significantly. After a critical value, the final AP population is eventually almost insensitive to any further increases in μ_{SCA}. With periodic infusion and with a* not conserved, even a more vigorous drug is not found to be effective at large value of τ_{drug}. On the contrary, when a* is conserved over the entire duration of therapy and μ_{SCA} is smaller than 0.04, the dependence of drug efficacy on μ_{SCA} is nearly identical for a wide range of τ_{drug} values (including for the case of continuous infusion).

6 Achieving the same treatment efficacy with periodic therapy for larger τ_{drug} periods requires relatively larger values of μ_{SCA}. However, if τ_{drug} exceeds a value of 200 h, an order of magnitude larger value of μ_{SCA} is required. Such treatment could become chemotherapeutically challenging.

REFERENCES

Al-Hajj M, Becker MW, Wicha M, Weismann I, Clark MF (2004) Therapeutic implications of cancer stem cells. *Curr. Opin. Genet. Dev.* **14**, 43–47.

Al-Hajj M, Clarke MF (2004) Self-renewal and solid tumor cells. *Oncogene* **23**, 7274–7282.

Bonifazi F, de Vivo A, Rosti G, Guilhot J, Trabacchi E, Hehlmann R, Hochhaus A, Shepherd PC, Steegmann JL, Kluin-Nelemans HC, Thaler J, Simonsson B, Louwagie A, Reiffers J, Mahon FX, Montefuso E, Alimena G, Hasford J, Richards S, Saglio G, Testoni N, Martinelli G, Tura S, Baccarani M (2001) Chronic myeloid leukaemia and interferon-alpha: a study of complete cytogenic responders. *Blood* **98**, 3074–3081.

Brenton JD, Carey LA, Ahmed AA, Caldas C (2005) Molecular classification and molecular forecasting of breast cancer: ready for clinical application. *J. Clin. Oncol.* **23**, 7350–7360.

Byrne HM (2003) Modeling avascular tumour growth. In: Preziosi L, ed. *Cancer Modeling and Simulation*, p. 75. London: Chapman & Hall/CRC.

Clarke MF (2004) At the root of brain cancer. *Nature* **432**, 281–282.

Cortes J, O'Brien S, Kantarjian H (2004) Discontinuation of imanitib therapy after achieving a molecular response. *Blood* **104**, 2204–2205.

Ganguly R, Puri IK (2006) Mathematical model for the cancer stem cell hypothesis. *Cell Prolif.* **39**, 3–14.

Hanahan D, Weinberg RA (2000) The hallmarks of cancer. *Cell* **100**, 57–70.

Huff CA, Matsui WH, Smith BD, Jones RJ (2006) Strategies to eliminate cancer stem cells: clinical applications. *Eur. J. Cancer* **42**, 1293–1297.

Huntly BJ, Gilliland DG (2005) Summing up cancer stem cells. *Nature* **435**, 1169–1170.

Jessell TM, Lumsden A (1997) Inductive signals and the assignment of cell fate in the spinal cord and hindbrain. In: Cowan WM, Jessell TM, Zipursky SL, eds. *Molecular and Cellular Approaches to Neural Development*, p. 290. Oxford: Oxford University Press.

Jones RJ, Matsui WH, Smith BD (2004) Cancer stem cells: are we missing the target. *J. Natl. Cancer Inst.* **96**, 583–585.

Komarova NL, Wadarz. D (2005) Drug resistance in cancer: principles of emergence and prevention. *PNAS* **102**, 9714–9717.

Lessard J, Sauvageau G (2003) Bmi-1 determines the proliferative capacity of normal and leukaemic stem cells. *Nature* **15**, 255–260.

Mackenzie IC (2005) Retention of stem cell patterns in malignant cell lines. *Cell Prolif.* **38**, 347–355.

Maddrey AM, Bergeron JA, Lombardo ER, McDonald NK, Mulne AF, Barenberg PD, Bowers DC (2005) Neuropsychological performance and quality of life of 10 year survivors of childhood medulloblastoma. *J. Neurooncol.* **72**, 245–253.

Mauro MJ, Druker BJ, Kuyl J, Kurilik G, Maziarz. RT (2003) Increasing levels of detectable leukaemia in imanitib treated CML patients with previously undetectable or very low levels of BCR-ABL. *Proc. ASCO* **22**, 569.

Mayer LD, Harasym TO, Tardi PG, Harasym NL, Shew CR, Johnstone SA, Ramsay EC, Bally MB, Janoff AS (2006) Ratiometric dosing of anticancer drug combinations: controlling drug ratios after systemic administration regulates therapeutic activity in tumour-bearing mice. *Mol. Cancer Ther.* **5**, 1854–1863.

Michor F, Hughes TP, Iwasa Y, Branford S, Shah N, Sawyers CL, Nowak MA (2005) Dynamics of chronic myeloid leukaemia. *Nature* **435**, 1267–1270.

Molofsky A, Pardal R, Iwashita T, Park I-K, Clarke MF, Morrison SJ (2003) Bmi-1 dependence distinguishes neural stem cell self-renewal from progenitor proliferation. *Nature* **425**, 962–967.

O'Brien SG, Guilhot F, Larson RA, Gathmann I, Baccarani M, Cervantes F, Cornelissen JJ, Fischer T, Hochhaus A, Hughes T, Lechner K, Nielsen JL, Rousselot P, Reiffers J, Saglio G, Shepherd J, Simonsson B, Gratwohl A, Goldman JM, Kantarjian H, Taylor K, Verhoef G, Bolton AE, Capdeville R, Druker BJ; IRIS Investigators (2003) Imanitib compared with interferon and low-dose cytarabine for newly diagnosed chronic-phase chronic myeloid leukaemia. *N. Engl. J. Med.* **348**, 994–1004.

O'Neill A, Schaffer DV (2004) The biology and engineering of stem cell control. *Biotechnol. Appl. Biochem.* **40**, 5–16.

Oliver TG, Wechsler-Reya RJ (2004) Getting at the root and stem of brain tumour. *Neuron* **42**, 885–888.

Pardal R, Clarke MF, Morrison SJ (2003) Applying the principle of stem cell biology to cancer. *Nat. Rev. Cancer* **3**, 895–902.

Pierce A, Smith DL, Jakobsen LV, Whetton AD, Spooncer E (2001) The specific enhancement of interferon alpha induced growth inhibition by BCR/ABL only occurs in multipotent cells. *Hematol. J.* **2**, 257–064.

Polakis P (2000) Wnt Signaling and cancer. *Genes Dev.* **14**, 1837–1851.

Polyak K, Hahn WC (2006) Roots and stems: stem cells in cancer. *Nat. Med.* **12**, 296–300.

Reya T, Morrison SJ, Clarke MF, Weissman IL (2001) Stem cells, cancer, and cancer stem cells. *Nature* **414**, 105–111.

Roeder I, Horn M, Glauche I, Hochhaus A, Mueller MC, Loeffler M (2006) Dynamic modeling of imatinib-treated chronic myeloid leukemia: functional insights and clinical implications. *Nat. Med.* **12**, 1181–1184.

Singh SK, Hawkins C, Clarke ID, Squire JA, Bayani J, Hide T, Henkelman RM, Cusimano MD, Dirks PB (2004) Identification of human brain tumor initiating cells. *Nature* **432**, 396–401.

Stordal BK, Davey MW, Davey RA (2006) Oxaliplatin induces drug resistance more rapidly than cisplatin in H69 small cell lung cancer cells. *Cancer Chemother. Pharmacol.* **58**, 256–265.

Taipale J, Beachy PA (2001) The Hedgehog and Wnt signaling pathways in cancer. *Nature* **411**, 349–254.

Viswanathan S, Zandstra P (2003) Towards predictive models of stem cell fate. *Cytotechnol.* **41**, 75–92.

Wichmann HE, Loeffler M (1984) *Mathematical Modeling of Cell Proliferation: Stem Cell Regulation in Hemopoiesis*, Vol. I. Boca Raton, FL: CRC Press.

